CHALMERS

Kollicoat IR/Brij 78: A stable couple?
Storage stability of aqueous pharmaceutical coatings

Master of Science Thesis

Johan Karlsson

Supervisor: Johan Hjärtstam, AstraZeneca, Mölndal
Examiner: Krister Holmberg

Department of Chemical and Biological Engineering
Division of Applied Surface Chemistry
CHALMERS UNIVERSITY OF TECHNOLOGY
Göteborg, Sweden, 2010

Kollicoat IR/Brij 78: A stable couple?
Storage stability of aqueous pharmaceutical coatings

JOHAN KARLSSON

Department of Chemical and Biological Engineering
Applied Surface Chemistry
Chalmers University of Technology
SE 412 96 Göteborg
Sweden
Telephone +46 (0)31 772 10 00

Kollicoat IR/Brij 78: A stable couple?

Storage stability of aqueous pharmaceutical coatings

JOHAN KARLSSON

Department of Chemical and Biological Engineering
Applied Surface Chemistry
CHALMERS UNIVERSITY OF TECHNOLOGY
Göteborg, Sweden 2010

Abstract

Aqueous polymer dispersions are preferable to use instead of organic polymer solutions for pharmaceutical coatings mainly to avoid environmental toxicity. To get good reproducibility of the coating, the polymer dispersion needs to be stable. The coating quality will be affected if there is aggregation of the aqueous polymer dispersion. To get stable polymer dispersions incorporation of surfactant is used. Dispersions of Eudragit NM30D and Kollicoat IR have been investigated with a weight fraction of Kollicoat IR between 5% and 25%, and these turned out to be stable throughout the entire analysis time of 4 months.

Another issue which could affect the quality of the coated membrane would be if the surfactant leaves the film. The hypothesis is that the surfactant, Brij 78, could form interactions with Kollicoat IR and this would by other words lead to a more stable surfactant impact. Therefore polymer coatings only containing Kollicoat IR and Brij 78 have been examined in this project. The results from analyses with polymer films of Kollicoat IR and Brij 78 show that there are interactions between them. When the coating is created, the surface is completely covered with Brij 78, but during the coalescence Brij 78 goes into the coating gradually. Depending on the coalescence time and how large the Brij 78 fraction is, it is possible to get a surface essentially free from Brij 78.

The degree of crystallinity for Brij 78 when Kollicoat IR is present has been investigated. It has been seen that the degree of crystallinity decreases gradually during the coalescence process. This means that Brij 78 gets more and more interactions with Kollicoat IR. In the coalescence process with only Brij 78, the degree of crystallinity remains constant. The standard deviation in the crystallinity studies did also decrease with the coalescence process, this trend shows that the films become more homogeneous during the coalescence process. Furthermore it has also been seen that there are interactions between Kollicoat IR and Brij 78 in solution.

Table of Contents

1   Introduction

1.1   Background

The purpose of using polymeric film as pharmaceutical coatings can be many: they can be applied to protect the active substance from exposure to light, moisture and oxygen, and they can mask unpleasant taste. In oral medicines, polymeric coatings can be used to get site specific release and also to get a controlled release [1]. By varying coating level, type of polymer and type and amount of plasticizer a desired drug release profile can be obtained, but variation of these parameters are generally restricted. A better approach to get a desired drug release profile is based on blending different polymers. Release patterns can be adjusted by changing polymer/polymer blend ratios [2]. To get a low permeability, water-insoluble polymer is used. This kind of polymer can be applied as organic solutions or aqueous colloidal dispersions. To increase the permeability, a water-soluble polymer is also added. The ratio between the water-insoluble and the water-soluble polymer can be adjusted to give desired modified release.
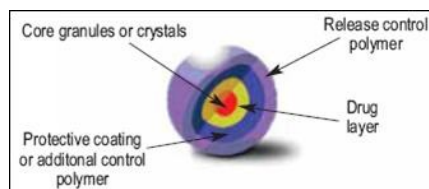

Figure 1.1: Artistic representation of layering technique
used for modified-release tablets.

The use of aqueous polymer dispersions instead of organic polymer solutions as pharmaceutical film coatings is preferable to avoid environmental toxicity. Another advantage with aqueous polymer dispersions is that the processing time can be reduced because of the higher polymer content in the dispersion of the coating [3] and hence a decrease of the process costs. Furthermore polymers used in aqueous dispersions are synthetic such as acrylics. In organic polymer solutions the polymers are usually based on cellulose derivates. Cellulose is a naturally organic compound and has a major problem in batch variations. An important issue of aqueous coatings is whether the aqueous dispersion is stable or not, i.e. do the polymer particles remain separated and dispersed in water or do they aggregate and settle out. The stability of the dispersion affects the storage time [4].

The film formation mechanism for aqueous polymer dispersions and organic polymer solutions differs. In an organic polymer solution, the polymers have a high mobility. When the solvent evaporates the polymer chains approach each other and form a continuous network, a polymer film. In aqueous polymer dispersion the polymers are deposited as small particles, polymer spheres. To achieve coalescence, the polymer spheres need to deform in order to get a continuous polymer film as the water evaporates. The driving force for coalescence comes from capillary forces caused by high interfacial tension between water and the polymers, and between water and air [5]. To get the individual particles to coalesce there needs to be appropriate conditions of temperature and water content. There are two major impacts of the presence of

water. One is that it can act as a plasticizer and therefore increase the mobility of the polymers giving an increased coalescence. The second is that it gives a capillary force driving the polymer particles together. The use of plasticizers is also important since it can reduce the minimum film-formation temperature. The use of a hydrophilic compound in the film can result in an improved film formation since it acts as a trap for water. Water then acts as a plasticizers and increases the capillary force which drives the polymer particles together. The film-forming mechanism from aqueous polymer can be divided into three stages: (I) evaporation and particle coalescence, (II) particle deformation and (III) particle-particle interdiffusion [6], this can be seen in figure 1.2. This more complex film formation for aqueous-based films may lead to differences in functional performance compared to organic-based films.
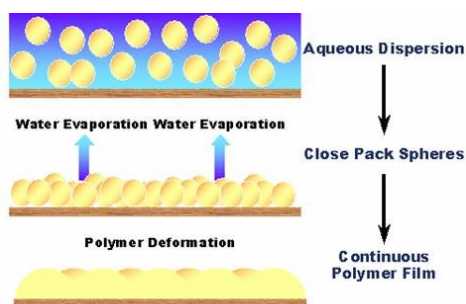

Figure 1.2: The three steps in the mechanism for film formation from aqueous polymer dispersion.

It is difficult to assure a complete film formation from aqueous polymer dispersions. To get complete polymer particle coalescence, generally a thermal-after-treatment, curing, is performed. Curing can be defined as the input of energy to the film system after the film has been applied [7]. An increase of temperature increases the mobility of the polymers which facilitate further coalescence [8]. An elevated relative humidity gives increased plasticizing affect and increased capillary forces. Depending on formulation factors such as the level of plasticizers and the coating conditions, the curing can be adjusted. The properties of the film change during coalescence. The structure of the film becomes denser and less permeable, which consequently gives decreased release rate [9]. Knowledge about the time and conditions for curing to achieve complete coalescence is needed to make sure that the properties of the coating are maintained during storage.

A major focus in the area of polymer films used to achieve modified release is the stability of the film. There is a correlation between the drug concentration in blood and the pharmaceutical effect of the drug [10], which can be seen in figure 1.3. If the film bursts after administration, it can give life-threatening side effects. There are several factors that can give film coat alteration during storage and therefore affect the stability. Migration of plasticizer and temperature in combination with a high humidity could affect the release after storage [11]. The unwanted adverse reactions will be reduced with greater control of the drug release rate.
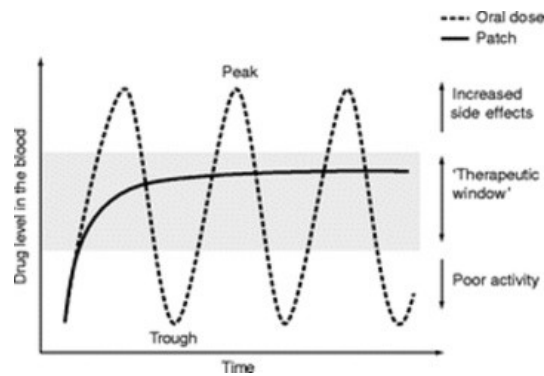
Figure 1.3: Illustration of therapeutic window.

In this master's thesis Eudragit NM30D is used as the water-insoluble polymer. This polymer is poorly permeable for water and most drugs. By only using this component as coating, the drug release may be too slow. To overcome this restriction Kollicoat IR is added. Kollicoat IR is used as the water-soluble polymer. It is in other words acting as a release modifier or pore maker. By using different ratios of these two polymers, the coating permeability can be tuned [12].

Surfactants are an important component to get particle stability in dispersions. Brij 78 is used as dispersion stabilizer in Eudragit NM30D. During aging, there is a risk that surfactants will migrate to the surface of the coating [13], and hence affect the release properties of the film. Therefore it is important to know the surfactant and polymer compatibility. When coatings of Eudragit NM30D and Kollicoat IR have been tested earlier as membranes, they have been shown to be stable. The hypothesis is that the surfactant, Brij 78, can form interactions with Kollicoat IR. Looking at the chemical structures of them, it would be possible that hydrogen bonds can be formed between them in the coating. The hypothesis can be seen in figure 1.4.
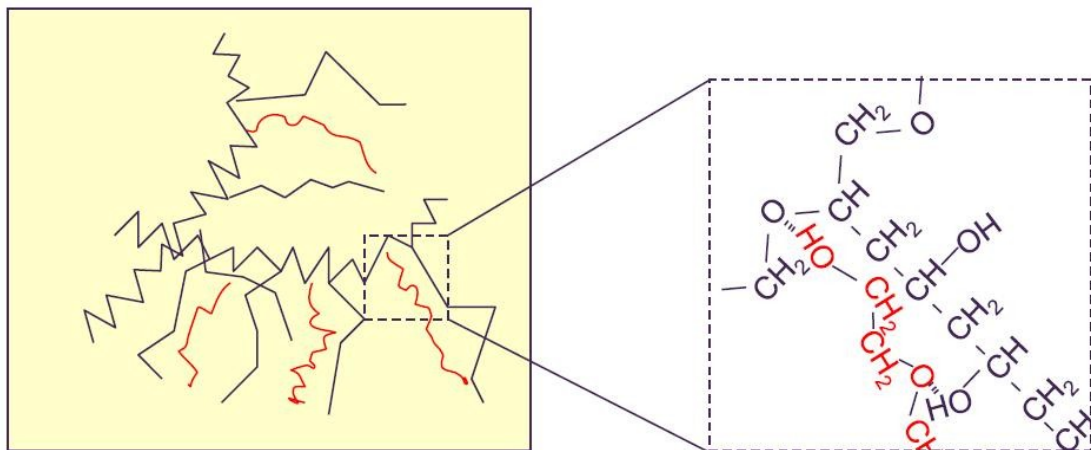
Figure 1.4: The hypothesis of interactions between Kollicoat IR and Brij 78. Kollicoat IR is illustrated with dark color and Brij 78 with red color.

1.2   Aim

The aim of this master's thesis can be divided into two parts. The primary aim is to examine if there exists interactions between Kollicoat IR and Brij 78. If Brij 78 would migrate out from the coating, leaving the coating, it could affect the release rate.

The secondary aim is to examine the dispersion stability of Eudragit NM30D together with Kollicoat IR. The stability of the dispersion is essential. Aggregation of the aqueous polymer dispersion would affect coating quality. This would affect the reproducibility of the polymer films.

2 Theory

2.1 Glass transition temperature

Semi-crystalline polymers contain both amorphous and crystalline regions. The amorphous region can be either a glassy or rubbery state depending on temperature. The temperature where the amorphous phase becomes converted from glassy to rubbery state is called glass transition temperature, T_g. At temperatures below T_g, the amorphous part is in its glassy state. In this region only small vibrations of short fragments will occur. In the glassy state polymers are generally stiff and brittle. When increasing the temperature above T_g to the rubbery state, molecules will start to wiggle, and the material becomes soft and flexible.

Thermodynamic transitions are classified into first- and second-order transition. The concept of first-order transition is that there will be heat transfer between the material and the surroundings and that the system will get an abrupt specific volume change. In second-order transitions there is no heat transfer, but there is a change of heat capacity. As the motion increases the specific volume increases. The glass transition is categorized as a second-order transition [14]. The physical properties that change drastically at T_g of any polymer are hardness, volume, modulus and percent elongation-to-break [15]. Due to changes in specific volume at T_g, the permeability of the film will be affected at this phase transition.

2.2 Melting and crystallization

Melting and crystallization are both phase transitions of first order [16]. They are phase transitions where the heat capacity as a function of time and temperature exhibits an abrupt specific volume change. When characterizing it with techniques that can detect thermal transitions, it will be presented as a peak. The peak area in the thermogram is directly proportional to the energy which is emitted or absorbed during the phase transition. Melting point, T_m, is the transition where the crystalline phase in the polymer becomes a disordered melt [17]. Melting is only a phenomenon for thermoplastics since thermosettings will decompose at high temperatures.

2.3 Differential Scanning Calorimetry

Differential Scanning Calorimetry, DSC, is a method used to study thermal transitions of polymers. The device consists of two heaters, and on top of these two pans are placed: one sample pan and one reference pan. The reference pan is often left empty. These pans are made of a metal with good heat conduction. A computer will assure that the temperature change of both pans will have the same rate. Since there is polymer in the sample pan, it will provide more energy than the reference pan. The temperature will be plotted against the heat flow. An exothermic change will give rise to a peak in the exothermic direction and an endothermic change will give rise to a peak in the endothermic direction [18]. The peak area is proportional to the total enthalpy change. The different peaks that can be seen in a DSC plot are glass transition temperature, T_g, crystallization temperature, T_c, and melting temperature, T_m. T_c and T_m will only be seen for polymers that contain a crystalline phase.

From the different phase transitions it is possible to investigate whether there are interactions between different components. Changes of temperature for different phase transitions and enthalpy values are indications that there are interactions between the components.

2.4 Atomic Force Microscopy

Atomic Force Microscopy, AFM, is today a leading scanning probe technique with broad applications. It is a surface sensitive method to analyze both chemical and biological surfaces. The main components in AFM are a piezo-ceramic scanner, a probe, a detector and associated electronics [19]. An AFM probe is usually a rectangular substrate which is typically 3.7 mm long and 1.8 mm wide, with a thickness around 0.5 mm. The probe supports a rectangular or triangular-shaped cantilever with a sharp vertical tip at one end. First the probe approaches the surface to a certain level of tip and sample interaction. The probe moves across the sample laterally, at every point the setpoint interaction is kept constant for the probe by the scanner. A laser beam deflection system is used, where a laser is reflected from the back of the cantilever to a position-sensitive detector. Between the tip and the sample there are both attractive and repulsive forces which are recorded. These interactions are calculated and from this calculation an image can illustrate the surface. The level of detection with AFM can be down to atomic scale features in some cases. It is the piezo-scanner with its high force sensitivity and the high precision motion which is the key to achieving the unique capabilities for surface imaging. There are a number of advantages with AFM. Its probe makes measurements in three dimensions. The presentation of the sample surface will then be three dimensional. AFM measures and presents images with sub-angstrom accuracy. Minimal sample preparation is needed, and vacuum is not required for the measurement. AFM can examine most materials in air, liquid and vacuum. Usually the sample can just be placed in the AFM by simply cutting into a suitable size before mounting. The only things that need to be considered are sample tilt and secure mounting. Securely mounting is very important because AFM is sensitive to small motions [20].

Different modes exist to fulfill requirements of specific applications. Contact mode, noncontact mode and tapping mode are the three most common. For contact mode a sharp tip is constantly adjusted by a feedback loop, and from this signal a piezoelectric actuator will maintain a constant contact of the tip to the surface. The tip slides on the sample, going up and down on the surface hills and valleys. The tip is attached to a cantilever which has a low spring constant since the tip is in hard conduct with the surface throughout the scan. The stiffness needs to be lower than the effective spring constant holding the atoms together. The spring constant for this mode is normally lower than 1 N/m. The detection can come from either the repulsive force between the tip and the sample or the deflection of the tip and this can be converted into an analog image. Operating in contact mode has been proven successful but it suffers some drawbacks. When it comes to softer surfaces, some hard surfaces, surfaces containing small particles or biological samples there is a risk of destroying the surface with contact mode. The solution has been to develop different modes. Tapping mode uses a cantilever which is oscillating while the tip scans the surface. This is a gentler method and can therefore be applied to softer surfaces. At

the bottom of each oscillation, the tip will gently touch the surface, this prevents damage of the surface. To minimize the risk that the tip gets stuck on the surface, typically very stiff cantilevers are used. The amplitude of the cantilever is generated from a piezoelectric actuator. By using a feedback loop, the amplitude will be maintained constant during the scan at the lowest possible level. When the tip passes a bump, there will be less room for oscillation and the amplitude decreases, and when passing a depression, the cantilever gets more room to oscillate and the amplitude becomes bigger. These differences are detected, and then a digital loop adjusts the tip-sample separation to maintain constant amplitude. In noncontact mode, the tip hovers 50-150 Å above the surface, in this regime the attractive Van der Waals forces are acting between the tip and the sample. Since these Van der Waals forces are fairly weak, the tip is given a small oscillation to be able to detect the small forces between the tip and the sample. The cantilever used for this mode is fairly stiff [21].

When examining polymer materials, AFM can visualize its surface topography, evaluate the surface roughness and correlate it with other surface characteristics such as optical properties, appearance and film formation. Compositional imaging for polymers can also be done with AFM. Individual components can be detected at a heterogeneous polymer surface since AFM can sense differences in properties. Because of that ability, mapping of domains can be done in AFM for semi-crystalline polymers, block copolymers, polymer blends and composite materials [22].

2.5   Time-of-Flight Secondary Ion Mass Spectrometry

Time-of-Flight Secondary Ion Mass Spectrometry, TOF-SIMS, is a surface analysis and chemical imaging method for solid samples. Chemical imaging is possible for both organic and inorganic species. A pulsed ion beam, with (in these studies) a Au source is emitted from an ion gun towards the surface, and when it hits the surface a collision cascade caused by these primary ions will eject molecules in the outermost layers [23]. These secondary ions will be identified on a mass basis, that is, their exact times through the flight path from the surface to the detector are measured. From this measurement, the mass can be determined. All kinds of elements and isotopes and both conductive and insulating materials can be characterized. To get a high mean free path in the flight path, ultrahigh vacuum system is used [24].

Close to the impact location of the beam the removed particles tend to be dissociated ions. Further away from the impact location these particles tend to be molecular compounds. TOF-SIMS has three different modes for analysis of the sample. It can give a mass spectrum of the different elemental and molecular species on a surface. Distribution of individual species can be presented as an image. The third mode is depth profile where it removes layer by layer and an elemental distribution of the depth is given. The first two modes mentioned above are just removing a fraction of the outermost monolayers of the surface. The analysis depth is restricted to the top 1-3 monolayers [25].

2.6 Critical Micelle Concentration

Surfactants tend to go to the surface or to form complexes in the bulk. This dynamics of the surfactant give interesting variations in the surface tension. At low surfactant concentration, the surfactant will adsorb to the surface. This will lower the surface tension of the water since their hydrogen bonds will be disrupted by the surfactant. The surface tension will continue to decrease as the surfactant concentration is increased since more surfactants will adsorb to the surface. At a certain concentration it will be more energetically favorable to form micelles. The surfactant unimers in solution will then start to form micelles [27]. This specific concentration is called critical micelle concentration, CMC. Beyond this point the surface tension will be almost constant. Micelle formation is an alternative to adsorption at interfaces in order to remove hydrophobic groups from contact with water [26]. By doing this the free energy of the system will be lowered. Micelles can be seen as reservoir for surfactant unimers.
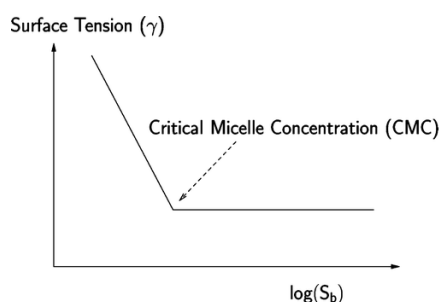

Figure 2.1: A characteristic appearance of a CMC curve.

2.7 Critical Association Concentration

Surfactants and polymer systems have a broad range of applications. Surfactants can be used in order to achieve colloidal stability, emulsification, flocculation and rheology control. The combination of polymer and surfactant can be used in diverse products such as cosmetics, paints, detergents and formulations of drugs. The effect on surface tension of a polymer at different surfactant concentrations will vary. At a certain concentration called critical association concentration, CAC, the surfactants will start to associate to the polymer. Below the CAC, the surface tension decreases as the surfactant adsorbs to the surface. The surface tension will be even lower than for the system with only surfactant since there will be some cooperation at the surface between the polymer and surfactant. Above the CAC the surface tension will remain constant for a range of increasing surfactant concentration, hence there will be no further increase in surfactant activity [26]. The length of this range will depend on the polymer concentration. Then at a certain surfactant concentration the surface tension will start to decrease again. At this point the polymer has become saturated with surfactant. Surfactant unimer concentration will increase which leads to an increased adsorption to the surface giving a decrease in surface tension. This continues until CMC is reached, after which the surface tension will stay constant and surfactant micelles will be formed [27].
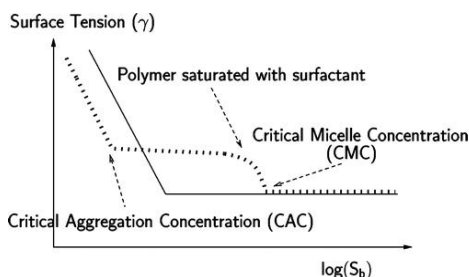
Figure 2.2: A system with polymer-surfactant interactions giving a CAC curve.

2.8 Wilhelmy plate method

In this method a platinum plate is used to investigate the surface tension. The platinum plate will function as the probe. The probe will first be wetted to a set depth that insures complete wetting, i.e., zero contact angle. Then it will be pulled upwards [28]. The position of the probe is significant and the force to pull the probe just at the interface will be recorded. From the registered force, the surface tension can be calculated. The equation used to calculate the surface tension is the following.

$$\sigma = \frac{F}{L \cdot \cos\theta}$$

Since the plate is optimally wetted the contact angle, θ, has the value of 0° which means that the term $\cos\theta$ equals the value 1. Therefore it is only the measured force and the length of the plate that need to be taken into consideration [29].

2.9 Thermogravimetric Analysis

Thermogravimetric Analysis, TGA, is mainly used to investigate the thermal and oxidative stability of materials [30]. During the measurement, the temperature is increased, and the sample weight is recorded continuously. The experiment is performed in a controlled atmosphere. At high enough temperatures, polymer decomposition will occur, providing information on the thermal stability. During the scan, different types of weight loss or gain can occur. Besides decomposition, there could be oxidation or dehydration [31]. This kind of analysis with temperature scanning is the most common procedure for TGA measurements and is called nonisothermal TGA. Isothermal measurements can also be performed where the weight is recorded over time at a constant temperature.

3   Materials and Methods

3.1   Materials

The purpose of this master's thesis is to investigate different properties for a pharmaceutical coating containing Eudragit NM30D, Kollicoat IR and PRUV.

3.1.1   Eudragit NM30D

Eudragit NM30D is an aqueous dispersion containing 30% of a copolymer of ethyl acrylate and methyl methacrylate. As emulsifier for the dispersion, 0.7% Macrogol Stearyl Ether (Brij 78) is used [33]. The dispersion has a milky-white color. It has a low viscosity and a faint characteristic odor. In a pharmaceutical polymer coating, it will be used as the water-insoluble component, and it has a low permeability. Its swelling is independent of pH. Other characteristics are that no plasticizers are required, and the coating from Eudragit NM30D has high flexibility. It has an approximate molecular weight of
600 000 g/mol. Its minimum film formation temperature is around 5°C, and the T_g is around 11°C. The CAS number is 9010-88-2, and the manufacturing company is Evonik Industries [34].
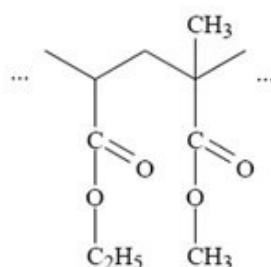

Figure 3.1: An illustration of a monomer for the copolymer in Eudragit NM30D.

3.1.2   Brij 78

Brij 78 is used as an emulsifier in the dispersion Eudragit NM30D. It is a nonionic surfactant with 20 PEG blocks. It is purchased from Aldrich [35]. The CAS number for Brij 78 is 9005-00-9. The molecular weight is 1151.57 g/mole [36]. It has a T_g of -39°C and T_m of 41.3°C. The melting enthalpy, ΔH_m, for Brij 78 is 165.8 J/g [32].
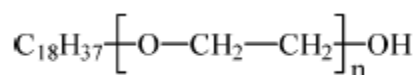

Figure 3.2: Schematic picture of Brij 78.

3.1.3   Kollicoat IR

Kollicoat IR was obtained from BASF (Ludwigshafen, Germany). It is a graft copolymer of polyvinyl alcohol, PVA, and polyethylene glycol, PEG. It is made for instant-release coating for tablets. In a coating mixed with a water-insoluble polymer,

it will be the pore former which determines the release rate. Kollicoat IR is a white free flowing powder which is soluble in water. The solubility is pH-independent since it has a nonionic structure and will therefore not be affected by the pH decreases and increases along the gastro intestinal tract [37]. Solutions of Kollicoat IR have low viscosity compared to other solutions of instant release polymers. It contains 75% PVA units and 25% PEG units. To improve the flow properties, it also contains 0.3% colloidal silica. The approximate molecular weight is 45 000 Daltons. The film coatings from Kollicoat IR are flexible and colorless. The surface tension of water will be reduced when Kollicoat IR is present. The aqueous solution will then be easy to spray and will give good wetting on the tablet surface. Its elongation break is much higher compared to cellulose derivates [38].
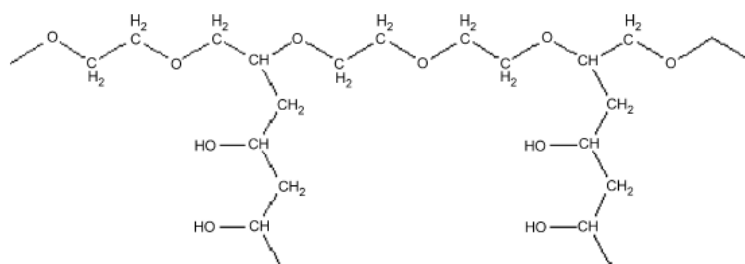
Figure 3.3: Chemical structure of Kollicoat IR.

3.1.4 PRUV

PRUV, Sodium Stearyl Fumarate, is normally used as a lubricant [39], but for this application it is used as an anti-sticking agent. Eudragit NM30D has a low T_g hence is an anti-sticking agent needed.
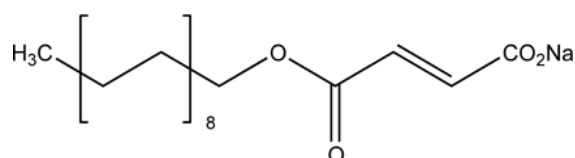
Figure 3.4: Chemical structure of PRUV.

3.2 Methods

3.2.1 Preparation of Suspension

3.2.1.1 Eudragit NM30D, Kollicoat IR and PRUV
The suspension of the overall system contain Eudragit NM30D, Kollicoat IR, PRUV and Milli-Q water. The amount of PRUV was determined to be 9 wt% of the total solid material. The ratio between the solid material in Eudragit NM30D and Kollicoat IR was changed between the films with specific intervals of 5 wt%. The different prepared ratios of solid material Eudragit NM30D/Kollicoat IR were: 100/0, 95/5, 90/10, 85/15, 80/20 and 75/25. To get 15 wt% solid material of Eudragit NM30D, Milli-Q water was added in the same amount as Eudragit NM30D.

The amount of Milli-Q water was weighed in a beaker, and then PRUV was added. This mixture was heated to 60°C and then cooled to room temperature during stirring of 600 rpm before Kollicoat IR was added. To get Kollicoat IR to dissolve in water only stirring (600 rpm) was needed. This mixture was stirred for at least 12 hours. The Eudragit NM30D was added to an E-flask and then the mixture of Milli-Q water, PRUV and Kollicoat IR was added. The entire mixture was stirred at 700 rpm for 30 minutes.

3.2.1.2 Kollicoat IR and Brij 78

The suspension contained 8 wt% Kollicoat IR and Brij 78 in Milli-Q water. Brij 78 is a solid gel at room temperature. Its melting point is about 41°C [32], and it was therefore put into a climate chamber at 60°C and 20%RH in order to be melted. Brij 78 was then added into a beaker containing the proper amount of water which had a temperature of 50°C. This mixture was stirred at 500 rpm for at least 30 minutes. Before adding Kollicoat IR the mixture was cooled down to room temperature. The amount of Kollicoat IR was then added to the mixture and stirred for at least an hour with a stirring rate of 600 rpm.

3.2.2 Dispersion stability of mixture of Eudragit NM30D and Kollicoat IR

To investigate the dispersion stability of Eudragit NM30D together with Kollicoat IR, a visual test was performed. The different ratios of Eudragit NM30D:Kollicoat IR were: 95:5, 90:10, 85:15, 80:20 and 75:25. The dispersions were prepared as mentioned above in beakers and then poured into different test tubes. The samples were stored at room temperature. Visual judgment was performed with intervals of 30 days.

3.2.3 Preparation of free polymer films

The preparation of free polymer films was done by spraying the suspension onto a rotating drum. The equipment can be seen in figure 3.5. The adjusted parameters were fluid flow (FF), fluid temperature (FT) and atomizer pressure (AP). The settings for these were: FF 40.0 m^3/h, FT 30.0°C and AP 2.00 bar. The suspension was sprayed onto a cylinder (drum) where the film formation occurs. The droplet size of the suspension that will be sprayed can be adjusted by changing the size of the nozzle. The nozzle moves back and forth, while the drum rotates to get an even film. The velocity of the nozzle's movement and the drum's rotation will determine how often the same area of the drum will be sprayed. Both the movement of the nozzle and the rotation of the drum had a voltmeter controlling the speed. The settings for the movement of the spray nozzle was 16 V and 0.4 A. The drum rotation was set to 5.1 V and 0.1 A. This gave a velocity of the nozzle and drum rotation of 1.3 cm/s and 80 rpm respectively. The distance between the spray nozzle and the drum was 100 mm.
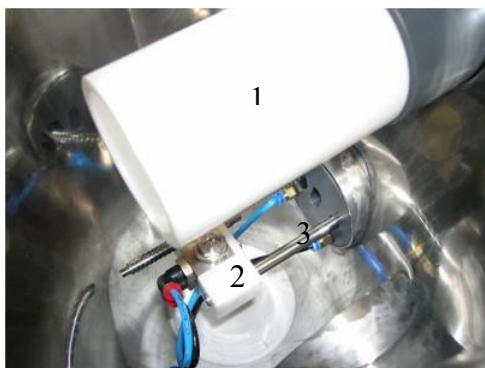
Figure 3.5: The equipment for spraying free films.
(1) Rotating drum, (2) spray nozzle and (3) moving arm.

Before the suspension is pumped into the system, it will be filtered to minimize the risk that particles get stuck in the hole of the nozzle. Water was first pumped into the apparatus and a few seconds later the suspension was added. The proper pumping rate of water could be chosen from the calibration that can be seen in figure 3.6.
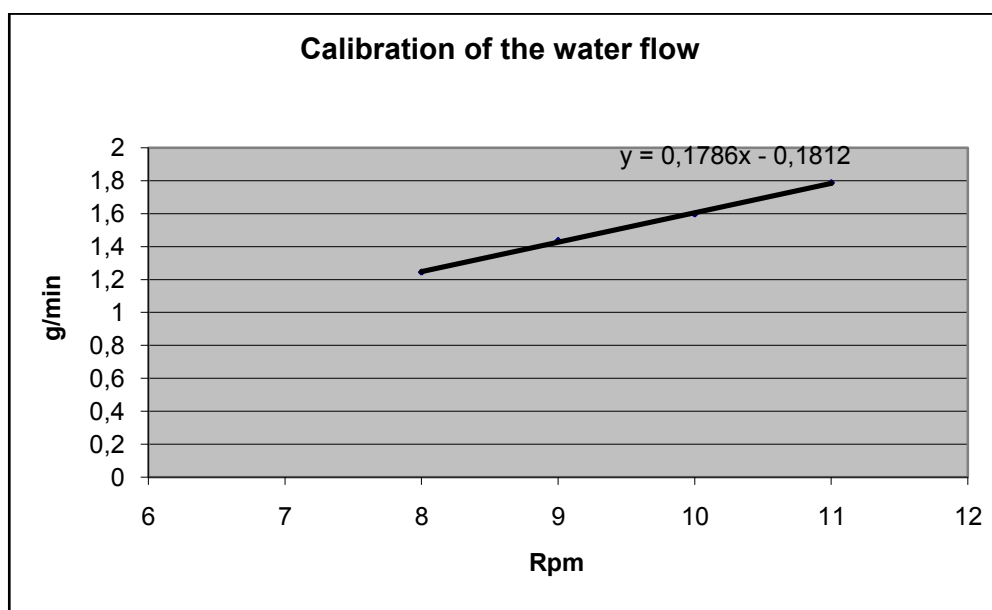

Figure 3.6: Calibration of the water flow.

The pumping rate of the suspension was set to 11 rpm. This setting gave good films with the parameters that were used. To make films that had a thickness of 120 μm, 19 g of the suspension was sprayed onto the drum. The processing time to spray 19 g was about 10 minutes. For DSC characterizations a thicker film was desired, and for these samples 50 g of the suspension was sprayed. The film was then peeled off the drum.

3.2.4   *Water permeability measurement*

The permeability apparatus contains two cell compartments, one donor and one receiver compartment. Between these cells there is a hole where the film is located. A small piece of free film was cut to cover the hole between the cell compartments. The thickness of each piece of the free film was measured at five different places. Before the experiment started was 15 ml of Milli-Q water added to both the cell compartments at the same time, to avoid any pressure on the membrane. There was a paddle in both the cell compartments to get good mixing, the speed of stirring was 200 rpm. To keep the temperature constant at 37°C in the cells throughout the experiment, a water jacket was used. In the beginning of each experiment 10 µl tritium water was added to the donor compartment. Samples of 500 µl were taken from the receiver compartment with specified time intervals, and when a sample was taken, 500 µl Milli-Q water was added to maintain the same volume in the receiver compartment. The samples were added into glass vials, and the radioactivity was later analyzed. To be able to detect the radioactivity, 4 ml of "Optiphase Hisafe 3" was added to the samples. Since "Optiphase Hisafe 3" is fairly viscous, properly shaking was important. The samples were standing in room temperature over the night to become homogenous. The samples were then analyzed by using a liquid scintillator counter, Winspectral^{TM} 1414 Liquid Scintillation Counter, which detected the radioactivity. From data of film thickness, sample weight, time when the sample was taken and radioactivity of the sample it was possible to calculate the permeability.

Two permeability tests could be done at the same time, and from them was the mean value calculated.
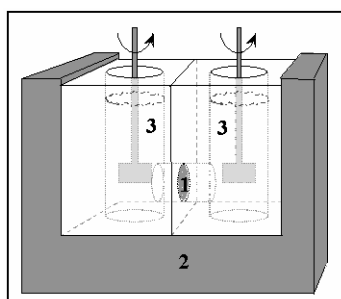

Figure 3.7: The apparatus of the permeability measurement: (1) where the film is located, (2) water jacket (37°C), (3) Donor compartment to the left and receiver compartment to the right.

Water permeability was examined for polymer films without curing and for films that had been cured. The curing was done in a climate chamber for 48 hours. The temperature and humidity was set to 60°C and 40%RH.

3.2.5 DSC characterization

Studies of the different phase transitions can indicate whether there are interactions or not between different components in a system, hence DSC is a suitable method to characterize if there is interactions between Kollicoat IR and Brij 78.

Aluminium sample pans of 50 µl were used. To get the polymer film into the sample pans, punching was done and these pieces were added to the sample pan to get around 10 mg samples. The exact weight was recorded. These samples were put in a desiccator containing a saturated salt solution of Lithium chloride. The condition inside this desiccator was 10.9%RH at room temperature. The low humidity was chosen to eliminate the influence of water. The samples were equilibrated for one week. When the samples were taken out, they were immediately sealed with hermetical covers to prevent any influence of the surroundings. The samples were weighed, and the sample weight was entered in the DSC experimental setup. Triplicate samples were analyzed.

The DSC was calibrated using indium and lead standards. The temperature scan for the samples was -40°C to 80°C at 20°C/min, followed by cooling from 80°C to -40°C at 20°C/min and then another heating cycle. The enthalpy of the melting peak for Brij 78 was then calculated.

3.2.6 AFM

The surface of the polymer films was analyzed with AFM to investigate if there is any migration of Brij 78. To get the high resolution which is possible, it is important that the surface is smooth, hence the way of making the films was important. Different methods for making the films were tested, but the most suitable was the one using an applicator. In this method, the solutions with different ratios of Kollicoat IR and Brij 78 were applied onto silicon plates using an applicator for 150 µm wet film thickness. The silicon plate with film was broken to get a small piece to fit in the AFM. The samples were imaged with 10×2.5 µm. Tapping/phase mode was used with 4096×1024-points/line resolution. The polynomial fit used to get the most distinct image was 2nd order for both topographic and phase contrast images. Both the surface topography and the surface composition were imaged. Phase imaging show both harder and softer areas, and varying in stickiness, and map them together with surface topography. Phase imaging is very sensitive and can reveal very thin layers that may not be seen in the topographic image. The analyzed surface was represented with both a topographic and a phase image. The different samples were analyzed both before and after curing. The curing was performed in a climate chamber with settings of 50°C and 60%RH for different amounts of time.

3.2.7 TOF-SIMS

Films that had been cast on silicon plates and analyzed in AFM were also analyzed with TOF-SIMS. In the method was an area of 100×100 µm characterized both in positive and negative mode. Gold was used as the ion source. The samples that were investigated can be seen in table 3.1.

Table 3.1: Samples carried out in TOF-SIMS.

Fraction Kollicoat IR/Brij 78	Time of coalescence in 50°C and 60%RH.
99/1	0 hours
99/1	3 weeks
90/10	0 hours
90/10	2 weeks

Kollicoat IR and Brij 78 were also analyzed by themselves as references. Kollicoat IR was analyzed just as powder. Brij 78 was prepared by first being melted in a climate chamber with a setting of 60°C, and then a droplet was added to a silicon plate.

3.2.8 Wilhelmy plate method

For analysis of the CMC for Brij 78 the Wilhelmy plate method was used. A solution of Brij 78 in Milli-Q water was prepared. The direction sheet of the method suggested preparing a solution with a concentration which is 150 times bigger than the expected CMC. In the literature the value is reported to be 5.7 µM [40], and from that value the concentration was decided to be 1 mM Brij 78 in the solution. This concentration appeared to give more points above CMC than below, therefore a concentration of 0.01 mM Brij 78 was also used. 10 ml Milli-Q water was added into a Petri dish. Into this Petri dish the solution of Brij 78 was titrated with a specific volume each time. The different added volumes can be seen in the table 3.2.

Table 3.2: The added volumes in the Wilhelmy plate method.

Added Volume (ml)	Total Volume (ml)
0,001	10,001
0,001	10,002
0,002	10,004
0,005	10,009
0,015	10,024
0,050	10,074
0,150	10,224
0,250	10,474
1,000	11,474
2,000	13,474
5,000	18,474

Stirring was applied after each titration and then the surface tension was measured. At each concentration the surface tension was measured five times and the mean value

was then calculated. When all analyses for the series were completed, surfactant concentration was plotted vs. surface tension.

Measurement to analyze if CAC exists for the system with Kollicoat IR and Brij 78 was also performed. The concentration of Kollicoat IR was 0.05 wt%. The Petri dish was filled with the solution of Kollicoat IR, and the titration solution with Brij 78 contained the same concentration Kollicoat IR as in the Petri dish in order to not dilute the polymer concentration. The same procedure as for the CMC measurement was then performed.

3.2.9   Thermogravimetric Analysis

Thermogravimetric analysis, TGA, measurement was carried out with the TGA Q500 from TA Instrument. In the method N_2 was used as purge gas to get a controlled atmosphere. A non-isothermal analysis was performed. The scan rate was 10°C/min going from room temperature to 350°C. 1.16 mg Brij 78 was added to the sample pan and then analyzed.

4   Results and discussion

4.1   Permeability for free films of Eudragit NM30D and Kollicoat IR

As expected the water permeability increased when the fraction of Kollicoat IR increased. The results are illustrated in figure 4.1.
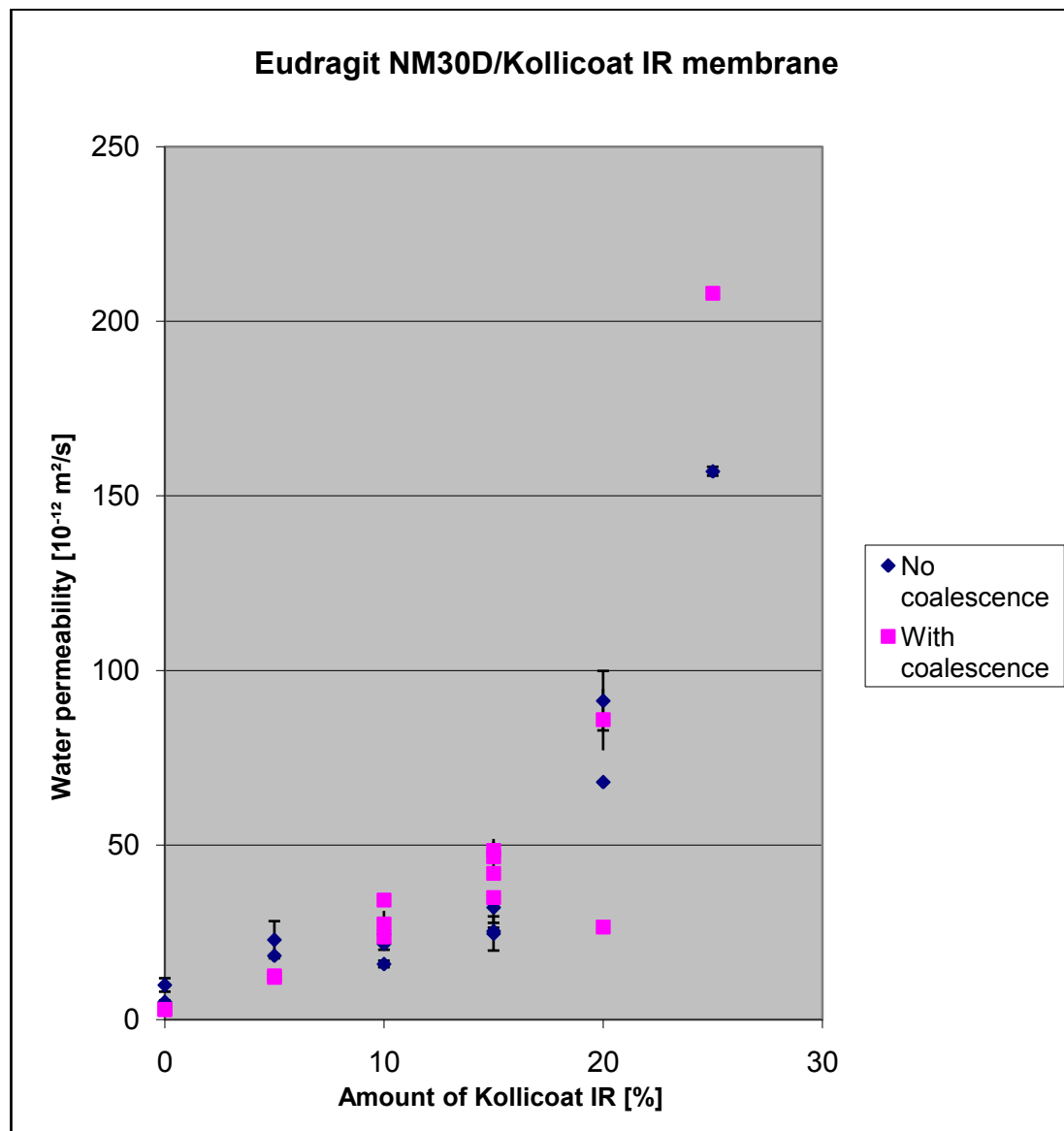

Figure 4.1: Water permeability for free films with different ratios of
Eudragit NM30D and Kollicoat IR.

For the cured free films there was a linear increase of water permeability up to the amount of 15 wt% Kollicoat IR. The trend that the water permeability increases with higher amount of Kollicoat IR continuous also for free films with both 20 and 25 wt% of Kollicoat IR, but there is an exponentially increase then. The films without curing do not have a linear trend, and this indicates that the cured films are more homogenous. It can also be seen that the standard deviation did decrease after

coalescence. This is another indication that the polymer films become more homogenous after coalescence.

4.2   Dispersion stability

Visual observation was performed every 30 day. Totally this investigation continued for four months, and during this time all the different dispersions proved to be stable. The results can be seen in table 4.1.

Table 4.1: The dispersion stability result for the different concentrations of Eudragit NM30D och Kollicoat IR.

Eudragit NM30D:Kollicoat IR (wt%)	Observation 1 month	Observation 2 months	Observation 3 months	Observation 4 months
95:5	Stable dispersion	Stable dispersion	Stable dispersion	Stable dispersion
90:10	Stable dispersion	Stable dispersion	Stable dispersion	Stable dispersion
85:15	Stable dispersion	Stable dispersion	Stable dispersion	Stable dispersion
80:20	Stable dispersion	Stable dispersion	Stable dispersion	Stable dispersion
75:25	Stable dispersion	Stable dispersion	Stable dispersion	Stable dispersion

4.3   DSC

There are four different phase transitions that could be analyzed with DSC for the mixture of Kollicoat IR and Brij 78. For both of them, T_g and T_m can be analyzed. Kollicoat IR has T_m at 209°C [41], but it is not possible to do a temperature scan in this area since Brij 78 can not stand such high temperature. T_g for both Kollicoat IR and Brij 78 are difficult to detect, since the inflection point is very small for both. The literature value of T_g for Brij 78 is -39°C [32], and for Kollicoat IR it is 37.4°C [42]. Even modulated DSC scans have been done for both Kollicoat IR and Brij 78 though the T_g was difficult to detect. The plots for modulated DSC scans for Brij 78 and Kollicoat IR can be seen in figure 4.2 and 4.3, respectively.
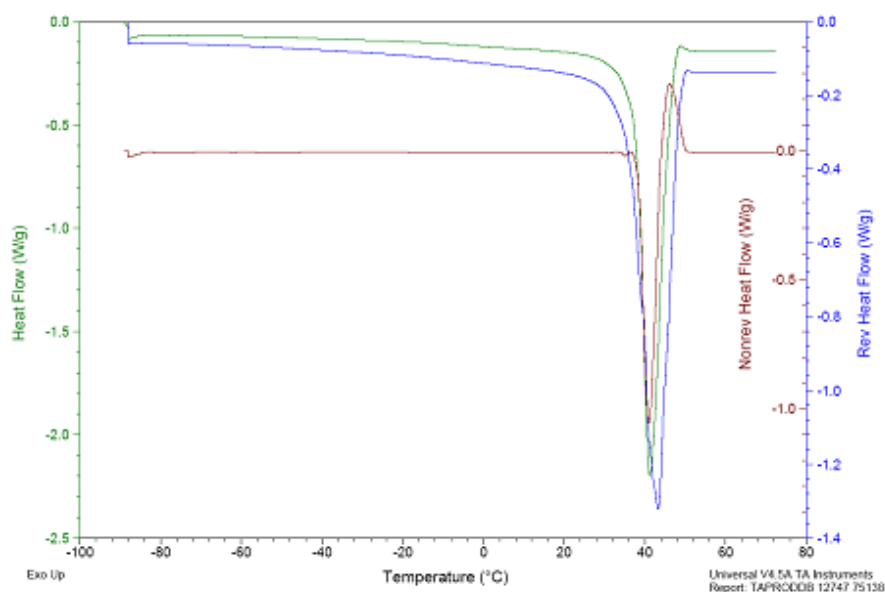
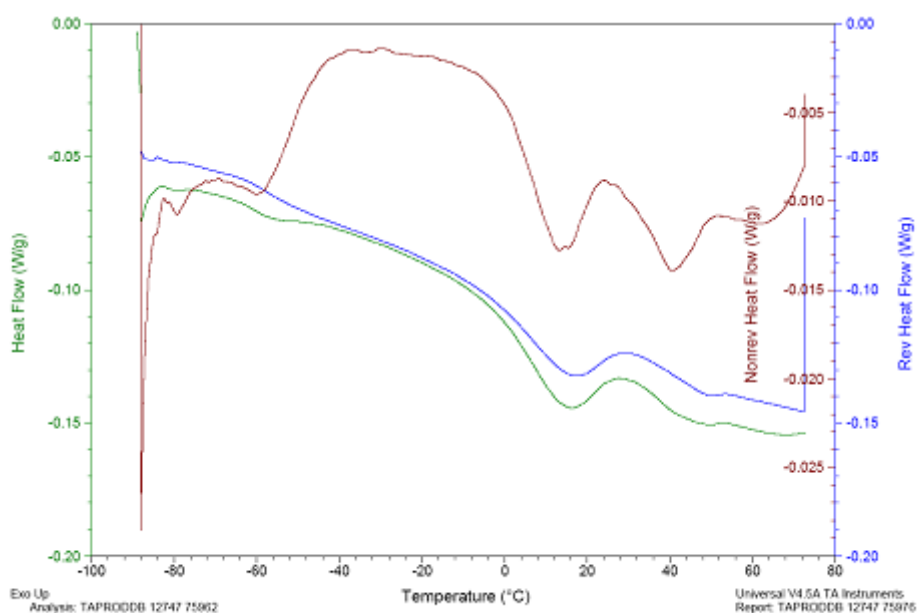Figure 4.2: Modulated DSC scan for Brij 78.

Figure 4.3: Modulated DSC scan for Kollicoat IR.

The T_m peak for Brij 78 is distinct, this can be seen in figure 4.2 just above 40°C. The melting enthalpy, ΔH_m, can be calculated. A decrease of ΔH_m would indicate interactions between Brij 78 and Kollicoat IR.

In figure 4.4 the studies of melting enthalpy can be seen. From the melting enthalpy, there is a trend that the crystallinity decreases when the coalescence time is increased, which indicate interactions between Kollicoat IR and Brij 78. Another interesting trend was that the standard deviation decreases at longer coalescence time. It seems like the films become more homogeneous during the coalescence process. This indication was also given from permeability analysis where the values of standard deviation became lower for coalesced films.
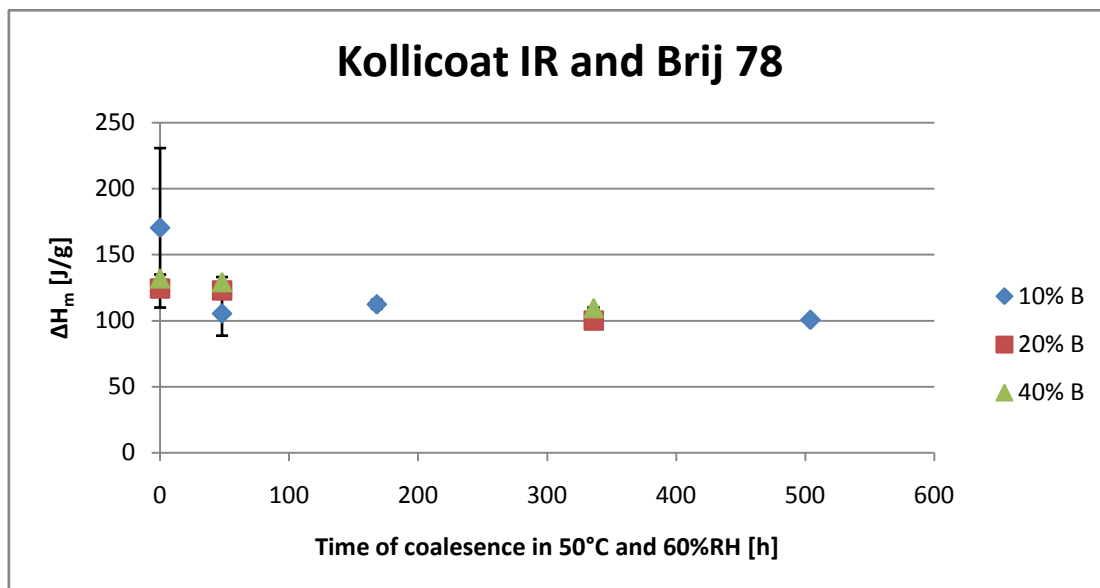
Figure 4.4: Melting enthalpies for Brij 78 in polymer films of Kollicoat IR and Brij 78.
The different fractions of Brij 78 were: 10%, 20% and 40%.
Times of coalescence can be seen on the x-axis.

Brij 78 was analyzed as a reference, and the result can be seen in table 4.2.

Table 4.2: Melting enthalpies for Brij 78 when Kollicoat IR was not present.

Time of coalescence (h)	Mean value $\Delta H_{m,B}$ (J/g)	St.dev. $\Delta H_{m,B}$ (J/g)
0	131,756	±8,471
48	133,127	±7,573

The results from the DSC scans with only Brij 78 show that there were no enthalpy changes during the time of coalescence. This indicates that no changes occur when Kollicoat IR is not present.

4.4   AFM

The coatings analyzed in AFM were Kollicoat IR/Brij 78: 99/1 and 90/10. In addition a coating containing only Kollicoat IR was analyzed to get a reference image.
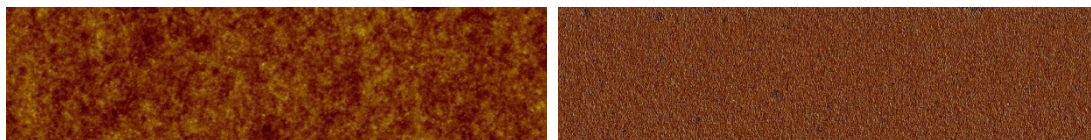

Figure 4.5: To the left is the height image. On its z-axis it is 10 nm from black to white. To the right is the phase image. Both images represent 100% Kollicoat IR 0h coalescence. Image size for each of them is 10×2.5 μm.

In figure 4.5 the Kollicoat IR surface is shown. From the topographic (height) picture a fine texture can be seen. That texture makes it easy to identify the Kollicoat IR surface. In the topographic image a small circular structure can be seen. The diameter of the circles has been measured with the software for AFM, and the average diameter was around 20 nm. The same structure can be seen in the phase image.

The Kollicoat IR film was put in climate chamber and AFM measurements were then made after 48 hours and 1 week, but no changes were seen. When comparing these images with the images from the coating with no coalescence time, the same fine texture was seen. The average size of the circular structures was still about 20 nm.
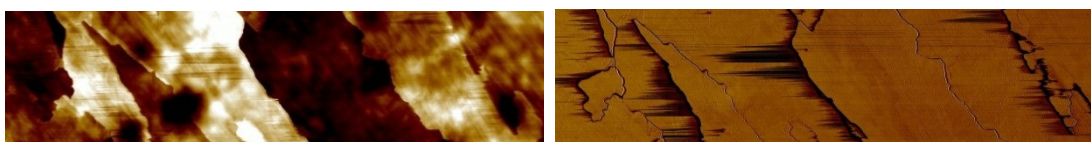

Figure 4.6: To the left is the height image. On its z-axis it is 40 nm from black to white. To the right is the phase image. Both images are representing Kollicoat IR/Brij 78 99/1 0h coalescence. Image size for each of them is 10×2.5 μm.

When adding just a fraction of 1% Brij 78 into the system, the AFM image was changed drastically. The surface became totally covered with Brij 78, and the fine texture from Kollicoat IR could not be seen, figure 4.6. In the topography image it can be seen that Brij 78 gives sharp edges, this is typical for a crystalline material. The color changes in the topographic image show that there are different amounts of Brij 78 layers at different locations. In the phase image in figure 4.6 there are no color changes which indicate that it is the same material covering the surface. The edges can be seen in the phase image, and around these there is some noise. This is because the edges are very sharp, and therefore it is difficult for the tip to follow the surface.
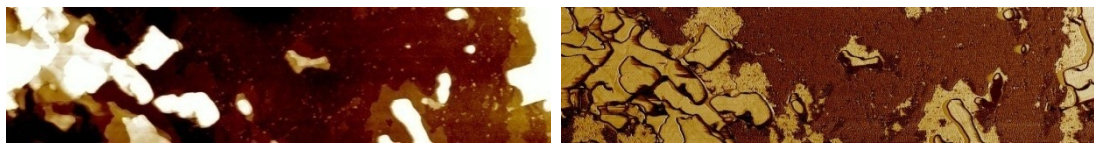
Figure 4.7: To the left is the height image. On its z-axis it is 10 nm from black to white. To the right is the phase image. Both images represent Kollicoat IR/Brij 78 99/1 1w coalescence, 50°C and 60%RH. Image size for each of them is 10×2.5 μm.

Figure 4.7 shows the surface for Kollicoat IR/Brij 78 99/1 when it has been in the climate chamber for 1 week, and there was a clear change of appearance for the surface. In the topographic image some fine texture has started to appear and the circular structure is about 20 nm, which was also observed for the pure Kollicoat IR surface. At some places no fine texture can be seen which means there are many layers of Brij 78 on top of Kollicoat IR surface. In the areas where some fine texture is observed, there is maybe just a monolayer left of Brij 78 which permits the Kollicoat IR texture to show through.

Looking at the same location in the phase image as in the topographic image the same pattern of circles can be seen at the same spot. This means that the topography is more dominant than the composition.
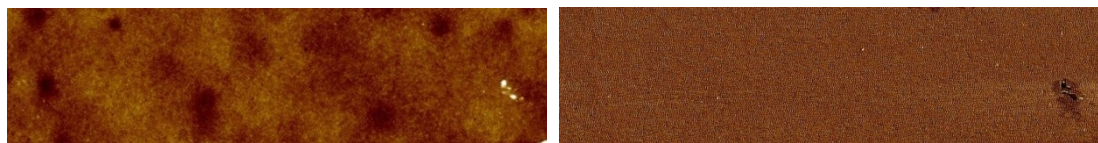

Figure 4.8: To the left is the height image. On its z-axis it is 10 nm from black to white. To the right is the phase image. Both images are representing Kollicoat IR/Brij 78 99/1 3w coalescence, 50°C and 60%RH. Image size for each of them is 10×2.5 μm.

After 3 weeks of coalescence the surface is almost totally covered with Kollicoat IR which could be seen in figure 4.8. The surface almost completely consists of a fine texture where the circles have a diameter of around 20 nm. There are just a few small spots left that represent Brij 78. These are seen as white spots. The phase image looks similar to the topographic image giving the same indications as the topographic image that the surface almost completely consists of Kollicoat IR.

Figure 4.9: To the left is the height image. On its z-axis it is 50 nm from black to white. To the right is the phase image. Both images represent Kollicoat IR/Brij 78 90/10 0h coalescence. Image size for each of them is 10×2.5 μm.

The surface of the film with 10% Brij 78 can be seen in figure 4.9. The z-axis is larger than before when just having 1% Brij 78. This means that there are many more layers of Brij 78 at some places. There was no tendency to see the Kollicoat IR surface.

Figure 4.10: To the left is the height image. On its z-axis it is 10 nm from black to white. To the right is the phase image. Both images represent Kollicoat IR/Brij 78 90/10 2w coalescence. Image size for each of them is 10×2.5 μm.

After 2 weeks of coalescence for the film with 10% f Brij 78, the fine texture started to appear again, figure 4.10. It did not appear as much as it did for the film with 1% Brij 78 after three weeks of coalescence. The fine texture was more easily seen in the phase image, but at the same spots where the fine texture can be seen in the phase image, it can also be seen in topography image. Thus some of the Brij 78 has moved into the bulk of the polymer film.

Characterization with AFM shows that the surface of coating with Kollicoat IR and Brij 78 was completely covered with Brij 78 when the films had been created. This could be due to the drying process. The surface of the film will dry last, at this moment there is low amount of water left. Brij 78 has a higher solubility than Kollicoat IR in water and it could therefore be that it is only Brij 78 present in the water that evaporates in the end. It could also be the higher mobility of Brij 78 which could be the reason why it will cover the surface of the coating. Kollicoat IR tends to be the dominate at the surface as the curing process proceeds. The goal for all systems are to lower the surface free energy, the explanation then would be that Kollicoat IR present at the surface decrease the surface free energy of the system.

4.5   TOF-SIMS

The results from polymer films of Kollicoat IR/Brij 78 90/10 and 99/1 have been compared with reference spectra of pure Kollicoat IR and Brij 78.
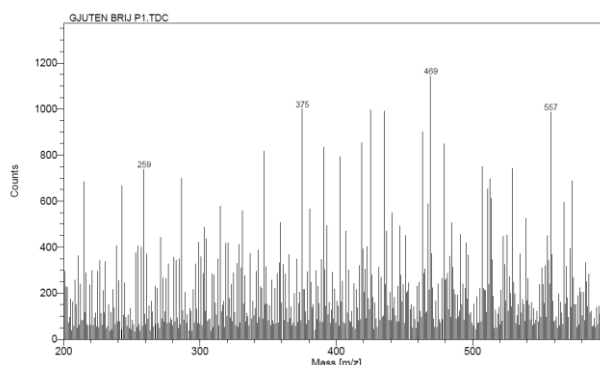

Figure 4.11: The result for Brij 78. The analysis was done in positive mode. The range presented is 200-600 m/z.

The spectra with pure Brij 78 can be seen in figure 4.11. Characteristic peak for Brij 78 is m/z 557.
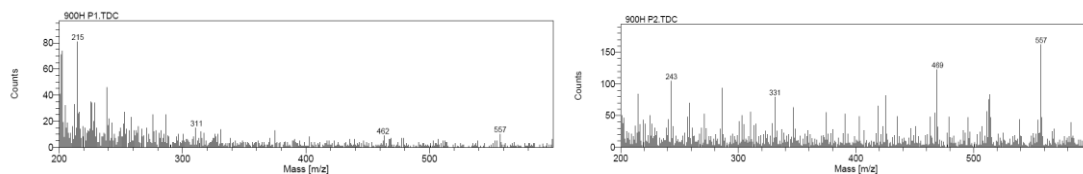
Figure 4.12: To the left is the spectrum for Kollicoat IR/Brij 78 90/10 0h coalescence at one location, and to the right is the spectrum for the same sample but at another location. Both analyses were done in positive mode. The range presented is 200-600 m/z.

In figure 4.12 the spectra for Kollicoat IR/Brij 78 90/10 before coalescence are shown for two different positions. These two spectra differ, indicating that the surface is inhomogeneous. When comparing with the Brij 78 reference in figure 4.12, it can be seen that some characteristic peaks for Brij 78 also exist in figure 4.12. Peak m/z 557 was seen at both positions. The intensity for the characteristic peak of Brij 78 is higher at position two than one. An explanation to the differences in the spectra between different positions could be that the surface was covered with a multilayer of Brij 78 at some places and not at others. Differences have been seen in AFM when it comes to layers of Brij 78 for surfaces covered with Brij 78.
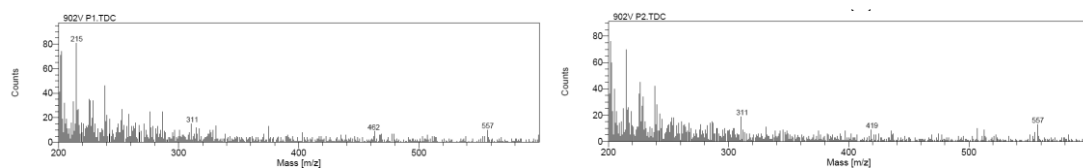

Figure 4.13: To the left is the result for Kollicoat IR/Brij 78 90/10 2 weeks coalescence in 50°C and 60%RH at one location and to the right is for the same sample but at another location. Both analyses were done in positive mode. The range presented is 200-600 m/z.

TOF-SIMS also showed that coalescence of the samples changes the composition at the surface. After 2 weeks of coalescence for coating with Kollicoat IR/Brij 78 90/10, results seen in figure 4.13, characteristic peaks for Brij 78 have decreased. Position one and two for the coating had very similar spectra. The coating seems to be homogenous. The characteristic peak for Brij 78 at m/z 557 has lower intensity after coalescence. The surface seems still to be occupied with Brij 78 but probably with fewer layers than before coalescence.
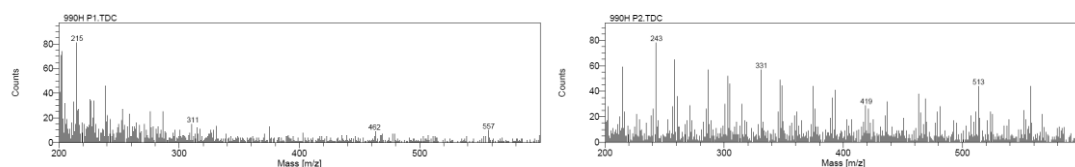

Figure 4.14: To the left is the result for Kollicoat IR/Brij 78 99/1 0h coalescence at one location, and to the right is for the same sample but at another location. Both analyses were done in positive mode. The range presented is 200-600 m/z.

Spectrum of coating Kollicoat IR/Brij 78 99/1 before coalescence, figure 4.14, contains also the characteristic peak for Brij 78 at m/z 557. When making comparison with the Kollicoat IR reference sample in figure 4.15, similarities could be seen but

the intensity for the peaks are much lower. The surface seems just to be partly occupied with Brij 78, or it could also be that there is just a monolayer of Brij 78 at some spots.
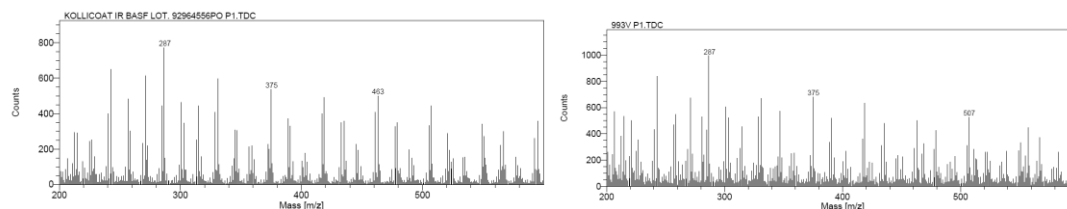

Figure 4.15: Pure Kollicoat IR was analyzed as reference and presented to the left. It was analyzed as powder. To the right is the result for Kollicoat IR/Brij 78 99/1 3 weeks coalescence in 50°C, and 60%RH. Both analyses were done in positive mode. The range presented is 200-600 m/z.

After 3 weeks of coalescence the Kollicoat IR/Brij 78 99/1 spectrum changed appearance compared to before coalescence. It has the same appearance as the Kollicoat IR reference spectrum, see figure 4.15. Brij 78 can not be seen after the coalescence. The surface completely corresponds to Kollicoat IR spectrum. This is what has been seen in AFM.
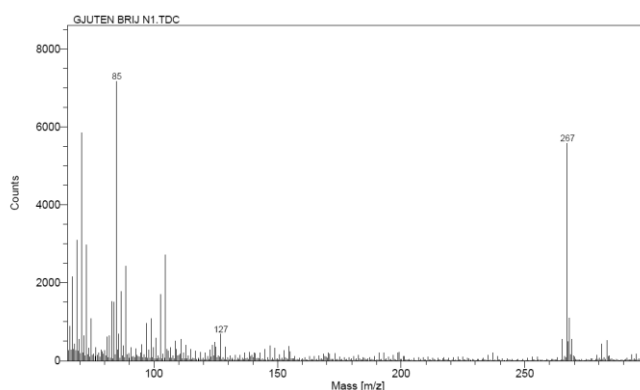

Figure 4.16: The result for Brij 78, in negative mode. The range presented is 0-300 m/z.

TOF-SIMS was also performed in negative mode. Characteristic peaks for Brij 78 in negative mode in the range up to 300 m/z are 85 and 267 m/z, these can be seen in figure 4.16.
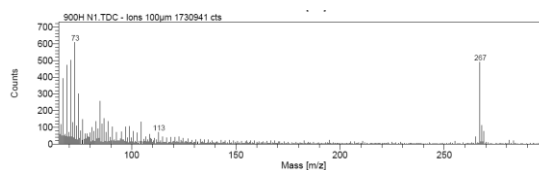

Figure 4.17: The result for Kollicoat IR/Brij 78 90/10 0h coalescence. The analysis was done in negative mode. The range presented is 0-300 m/z.

The spectrum in positive mode for Kollicoat IR/Brij 78 90/10 before coalescence showed that the surface was covered with Brij 78. The same thing was also seen in

negative mode. The peak at 267 m/z can clearly be seen in the spectrum for coating with Kollicoat IR/Brij 78 90/10 before coalescence, figure 4.17.
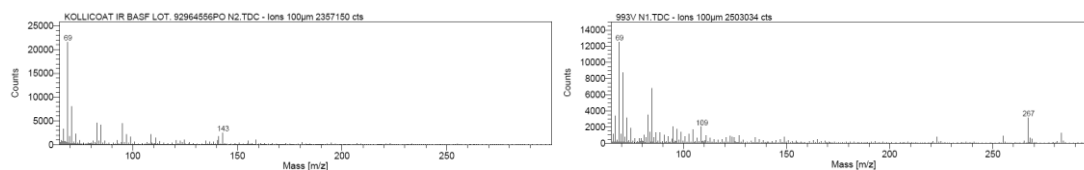

Figure 4.18: Pure Kollicoat IR was analyzed as reference and presented to the left. It was analyzed as powder. To the right is the result for Kollicoat IR/Brij 78 99/1 3 weeks coalescence in 50°C and 60%RH. Both analyses were done in negative mode. The range presented is 0-300 m/z.

Earlier analyses for the coating of Kollicoat IR/Brij 78 99/1 3 weeks coalescence had indicated that its surface mostly contains Kollicoat IR, and the same thing was seen in negative mode. The most characteristic peak for the Kollicoat IR reference is m/z 69, figure 4.18. This peak was also the peak which had the highest intensity in the spectrum for Kollicoat IR/Brij 78 99/1 3 weeks of coalescence. In this spectrum the peak m/z 267 could also be seen which indicates that there still exists some Brij 78 at the surface. The intensity for this was not as high, and the rest of the pattern corresponded to the Kollicoat IR spectrum.

4.6 Wilhelmy plate method

Wilhelmy plate method was done in order to see if interactions between Kollicoat IR and Brij 78 occurred in solution. The indication that interactions between them exist in solution would be if the system had a CAC. First surface tension was measured for only Brij 78 in order to find out its CMC value. The CMC value for Brij 78 was 5.0 µM, which can be seen in figure 4.19. This CMC value corresponds well to the literature value that was 5.7 µM [40]. When doing measurements with Kollicoat IR and Brij 78, it turned out that Kollicoat IR was fairly surface active itself. The first tested solution of Kollicoat IR 0.5% w/w had 50.3 mN/m in surface tension. A higher surface tension would be preferable. The concentration 0.05% w/w of Kollicoat IR turned out to be more suitable. This solution had 60.7 mN/m in surface tension. 0.05% w/w is a low polymer concentration, and this did probably bring that the CAC plateau became short. A CAC for the system was seen at 1.3 µM. This indicates that interactions exist between Kollicoat IR and Brij 78.
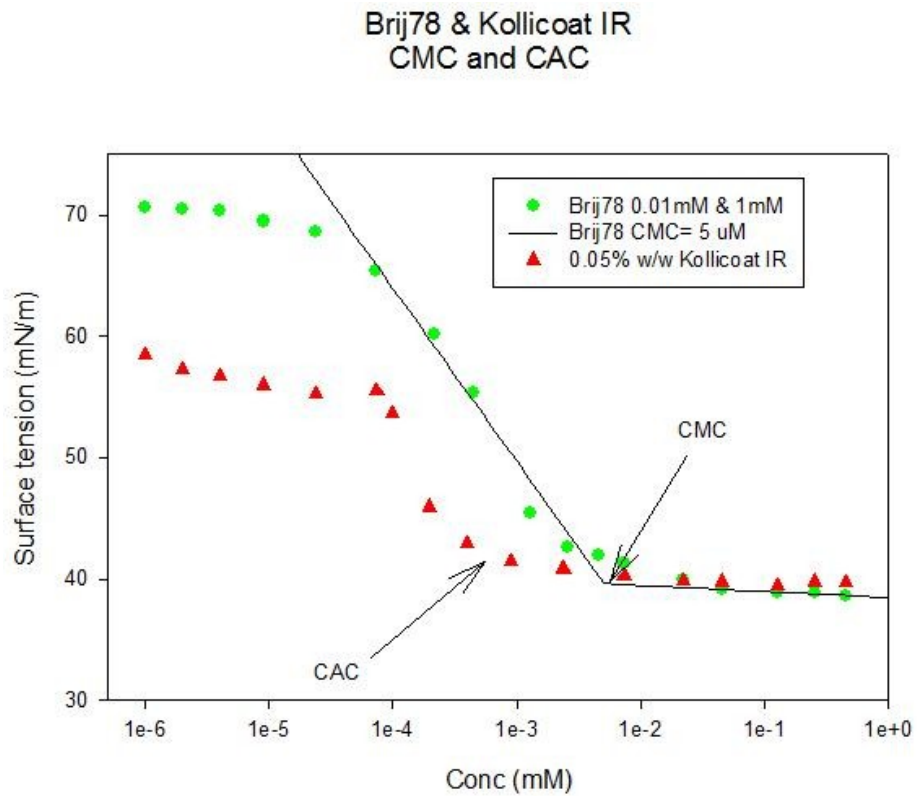
Figure 4.19: Results from Wilhelmy plate method. One series with only Brij 78 present and one series where 0.05% w/w Kollicoat IR present together with Brij 78.

4.7   TGA

From the AFM characterization results, it was seen that Brij 78 disappeared from the surface during coalescence. Either it could evaporate from the surface or it could go into the bulk of the polymer film. To investigate if the Brij 78 had evaporated or not, TGA measurement was performed. The TGA characterization showed that Brij 78 had a weight loss from around 180°C. In the temperature interval between room temperature and 200°C the weight loss was only 0.252%. This can be seen in figure 4.20. There should be no weight loss of Brij 78 during the coalescence at 50°C and 60%RH.
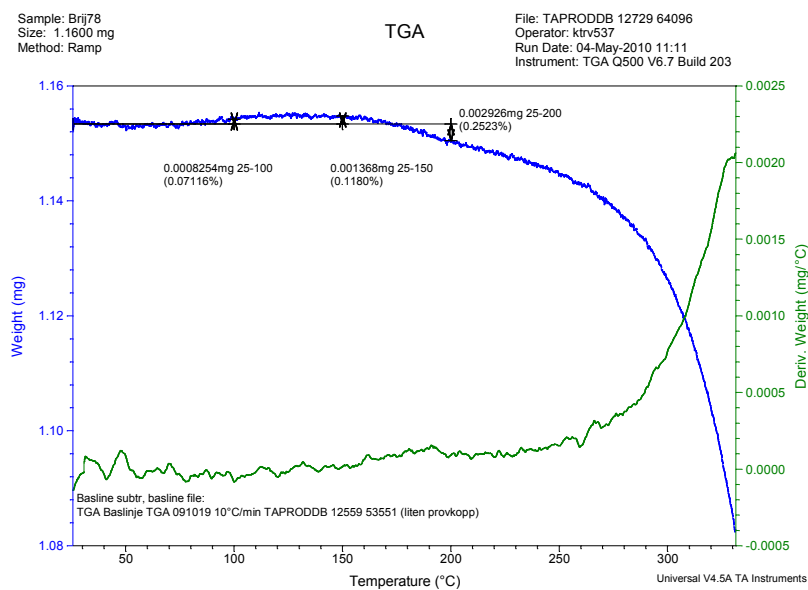

Figure 4.20: The result from the TGA characterization of Brij 78.

5   Conclusions

All different characterization methods have indicated that there exist interactions between Kollicoat IR and Brij 78.

From AFM measurements it was very obvious that the surface of the coating change during the curing process. At first when the coatings of Kollicoat IR and Brij 78 were created, their surfaces were completely covered with Brij 78. During the coalescence Kollicoat IR started to appear more and more. TGA analysis showed that Brij 78 has no weight loss at 50°C, which was the temperature in the curing process. This means that Brij 78 moves into the coating during the curing process. In both AFM and TOF-SIMS it could be seen that the surface for Kollicoat IR/Brij 78 99/1 with 3 weeks coalescence had a Kollicoat IR surface, essentially free from Brij 78.

The crystallinity of Brij 78 was studied with DSC, and the crystallinity decreased during coalescence when Kollicoat IR was present. This is an indication that interactions exist between Brij 78 and Kollicoat IR. The curing process also tends to make the films more homogenous. The standard deviations in the DSC measurement decreased as the time of the curing process increased.

Interactions also exist between Kollicoat IR and Brij 78 when they are mixed in water. From surface tension measurement a CAC could be identified for the system. From these measurements it could also be seen that Kollicoat IR is a surface active polymer.

To get a modified release Eudragit NM30D will be included as the water-insoluble component. The dispersion with Eudragit NM30D and Kollicoat IR in water turned out to be stable. Storage stability was tested for 4 months, and the dispersion was stable during the whole time. The reproducibility when creating the coating will not be affected by dispersion stability.

6   Future work

It has been seen in this master's thesis that there are interactions between Kollicoat IR and Brij 78. In the characterization methods used, it is not possible to see what kind of interactions is present. Using a suitable characterization method for this system would be interesting. Diffusion-NMR could maybe be a suitable method.

Thermal-after-treatment, curing, is a very important step when producing pharmaceutical coatings. Optimization of the curing process will be important in order to get a final product.

The maximum fraction Brij 78 which could interact with Kollicoat IR without getting an excess of Brij 78 would be an interesting property to know.

It would be interesting to investigate the cross-section of the coating in order to study the dynamics of Brij 78, in other words to follow the Brij 78 moving into the coating during coalescence. Also the packing of the different components in the film would be useful to understand.

7   Acknowledgements

I would like to thank the people that giving me such a great support during my master's thesis.

Thanks to:

Johan Hjärtstam, my supervisor, for your support, inspiration and effort in making this an interesting time for me. You have always been around for questions.

Mark Nicholas, for teaching and helping me with AFM and TOF-SIMS characterization. I appreciate all the discussions we had when interpreting the results.

Hanna Matic, for teaching and helping me with AFM and TGA. I have learnt a lot from the discussions that I had with you and Mark.

Christian von Corswant, for your support and the discussions that we had during the project about the results.

Pia Skantze, for teaching and helping me with the Wilhelmy plate method.

Hans Carlsson, for teaching and helping me with DSC characterization.

Mona Lina, for your help with modulated DSC characterization.

Staffan Schantz, for your support, and for taking time for questions.

Everybody in the OCR group at AstraZeneca, Mölndal. I did really feel like a team member in your group.

Krister Holmberg, my examiner, for all your support.

8   Bibliography

[1] Kranz, H. and Gutsche, S. (2009) *Evaluation of the drug release patterns and long term stability of aqueous and organic coated pellets by using blends of enteric and gastrointestinal insoluble polymers*. International Journal of Pharmaceutics, no. 380, pp. 112-119.

[2] Dashevsky, A., Ahmed, A. R., Mota, J., Irfan, M., Kolter, K. and Bodmeier, R. A. (2010) *Effect of water-soluble polymers on the physical stability of aqueous polymeric dispersions and their implications on the drug release from coated pellets*. Drug Development and Industrial Pharmacy, no. 36, pp. 152-160.

[3] Lecomte, F., Siepmann, J., Walther, M., MacRae, R. and Bodmeier, R. (2004) *Polymer Blends Used for the Coating of Multiparticulates: Comparison of Aqueous and Organic Techniques*. Pharmaceutical Research, Vol. 21, no. 5, pp 882-890.

[4] Guo, H. X., Heinämäki, J. and Yliruusi, J. (2008) *Stable aqueous film coating dispersion of zein*. Journal of Colloidal and Interface Science, no. 322, pp. 478-484.

[5] Mendoza-Romero, L., Piñón-Segundo, E., Nava-Arzaluz, M. G., Ganem-Quintanar, A., Cordero-Sánchez, S. and Quintanar-Guerrero, D. (2009) *Comparison of pharmaceutical films prepared from aqueous polymeric dispersions using the cast method and the spraying technique*. Colloids and Surfaces A: Physicochemical and Engineering Aspects, no. 337, pp. 109-116.

[6] Williams III, R. and Liu, J. (2000) *Influence of processing and curing conditions on beads coated with an aqueous dispersions of cellulose acetate phthalate*. European Journal of Pharmaceutics and Biopharmaceutics, no. 49, pp. 243-252.

[7] Muschert, S., Siepmann, F., Cuppok, Y., Leclercq, B. and Siepmann, J. (2009) *Improved long term stability of aqueous ethylcellulose film coatings: Importance of the type of drug and the starter core*. International Journal of Pharmaceutics, no 368, pp. 138-145.

[8] Muschert, S., Siepmann, F., Leclercq, B., Carlin, B. and Siepmann, J. (2009) *Prediction of drug release from ethylcellulose coated pellets*. Journal of Controlled Release, no. 135, pp. 71-79.

[9] Hamed, E. and Sakr, A. (2003) *Effect of curing conditions and plasticizer level on the release of highly lipophilic drug from coated multiparticulate drug delivery system*. Pharmaceutical Development and technology, Vol. 8, no. 4, pp. 397-407.

[10] Hjärtstam, J. (1998) *Ethyl Cellulose Membranes used in Modified Release Formulations*. PhD thesis, Chalmers University of Technology, Göteborg.

[11] Ensslin, S., Moll, K. P., Haefele-Racin, T. and Mäder, K. (2009) *Safety and robustness of coated pellets: self-healing film properties and storage stability*. Pharmaceutical Research, Vol. 26, no. 6, pp. 1534-1543.

[12] Siepmann, F., Muschert, S., Leclercq, B., Carlin, B. and Siepmann, J. (2008) *How to improve the storage stability of aqueous polymeric film coatings*. Journal of Controlled Release, no. 126, pp. 26-33.

[13] Schantz, S., Carlsson, H., Andersson, T., Erkselius, S., Larsson, A. and Karlsson, O.J. (2007) *Poly(methyl methacrylate-co-ethyl acrylate) Latex Particles with Poly(ethylene glycol) Grafts: Structure and Film Formation*. Langmuir, no. 23, pp. 3590-3602.

[14] http://faculty.uscupstate.edu/llever/Polymer%20Resources/GlassTrans.htm, (citied: 2010-01-21)

[15] http://www.msm.cam.ac.uk/phasetrans/2002/Thermal2.pdf, (citied: 2010-01-26)

[16] http://chem.chem.rochester.edu/~chem421/propsmw.htm, (citied: 2010-05-30)

[17] http://www.friedli.com/research/PhD/Dsc/chap3.html, (citied: 2010-01-26)

[18] http://web.missouri.edu/~kattik/katti/Thermal%20Behavior%20of%20Polymers.pdf, (citied: 2010-01-25)

[19] http://www.nanoscience.com/education/AFM.html, (citied: 2010-01-26)

[20] Blanchard, C. (1996) *The Chemical Educator: Atomic Force Microscopy*. Vol. 5, no. 5, pp. 1-8. New York: Springer Verlag.

[21] http://www.chembio.uoguelph.ca/educmat/chm729/afm/details.htm, (citied: 2010-02-01)

[22] Chernoff, D. and Magonov, S. *Comprehensive Desk Reference of Polymer Characterization and Analysis, Ch 19: Atomic Force Microscopy*. Ed: Brady, R., Oxford University Press, New York.

[23] http://serc.carleton.edu/research_education/geochemsheets/techniques/ToFSIMS.html, (citied: 2010-02-08)

[24] http://www.ammrf.org.au/docs/factsheets/FShip_ToFSIMS_UniSA_09w.pdf, (citied: 2010-02-09)

[25] http://www.phi.com/surface-analysis-techniques/tof-sims.html, (citied: 2010-02-09)

[26] http://pubs.acs.org/doi/full/10.1021/la063714h, (citied: 2010-05-19)

[27] Holmberg, K., Jönsson, B., Kronberg, B. and Lindman, B. (2007) *Surfactants and polymers in aqueous solution*, (2nd.ed), Chichester: John Wiley & Sons.

[28] http://www.attension.com/surface-tension.aspx, (citied: 2010-05-18)

[29] http://www.kruss.de/en/theory/measurements/surface-tension/plate-method.html, (cited: 2010-05-19)

[30] http://lww.kt.dtu.dk/~vigild/2005_04_melitek/tga.htm, (cited: 2010-05-25)

[31] http://membrane.ces.utexas.edu/Home/LabPractice/TGA.ppt, (cited: 2010-05-26)

[32] Fernandes, E. G., Krauser, S., Samour, C. M. and Chiellini, E. (2000) *Symmetric block oligomers, Gelation characteristics by DSC*. Journal of Thermal Analysis and Calorimetry, Vol. 61, no. 2, pp. 551-564.

[33] http://eudragit.evonik.com/sites/dc/Downloadcenter/Evonik/Product/EUDRAGIT/Specification%20EUDRAGIT%C2%AE%20NM%2030%20D.pdf, (cited: 2010-05-31)

[34] http://eudragit.evonik.com/product/eudragit/en/products-services/eudragit-products/sustained-release-formulations/nm-30-d/pages/default.aspx, (cited: 2010-05-31)

[35] Bronstein, L., Dixit, S., Tomaszewski, J., Stein, B., Svergun, D., Konarev, P., Shtykova, E., Werner-Zwanziger, U. and Dragnea, B. (2006) *Hybrid Polymer Particles with a Protective Shell: Synthesis, Structure, and Templating*. Chemistry of Materials, Vol. 18, no. 9, pp. 2418-2430.

[36] http://www.sciencelab.com/xMSDS-BRIJ_78-9923139, (cited: 2010-05-31)

[37] Janssens, S., de Armas, H. N., Remon, J. P. and den Mooter, G. V. (2007) *The use of new hydrophilic polymer, Kollicoat IR, in the formulation of solid dispersions of Itraconazole*. European Journal of Pharmaceutical Science, Vol. 30, no. 3-4, pp. 288-294.

[38] http://www.makeni.com.br/Portals/Makeni/prod/boletim/Kollicoat%20IR.pdf, (cited: 2010-05-31)

[39] http://www.jrs.de/wEnglisch/produkte/pruv.shtml, (cited: 2010-05-31)

[40] Hait, S. K. and Moulik, S. P. (2001) *Determination of Critical Micelle Concentration (CMC) of Nonionic Surfactants by Donor-Acceptor Interaction with Iodine and Correlation of CMC with Hydrophile-Lipophile Balance and Other Parameters of the Surfactants*. Journal of Surfactant and Detergents, Vol. 4, no. 3, pp. 303-309.

[41] Kolter, K., Gotsche, M. and Schneider, T. (2002) *Physicochemical Characterization of Kollicoat IR*. BASF ExAct, no. 8, pp. 2-3.

[42] http://141.48.65.167/diss-online/08/09H001/t2.pdf, (citied: 2010-05-12)